Phase Aspects and Localization Analysis of the Auditory N100 Component

G. Zouridakis, D. Iyer

Biomedical Imaging Lab, Department of Computer Science
University of Houston, TX, USA

Abstract—**The structure of the sources underlying surface recordings of brain activity is very complex. We have developed an iterative procedure based on independent component analysis to obtain single-trial estimates of the auditory N100 component recorded in normal subjects using a pure tone, binaural stimulation task and a whole-head, 256-channel recording system. For each channel, the processed single trials were separated into two groups, one with trials in which the N100 component had the same phase as the average response and another one with trials having the opposite phase. Our results show that the proposed method can effectively extract only the activity related to the experimental task, while removing artifacts and background activity, and that the sources of the N100 component that are typically localized on the floor of the Sylvian fissure are primarily due to in-phase responses.**

Keywords—**Independent component analysis, Source localization, Component phase, Evoked potentials.**

I. Introduction

Electric source imaging is a noninvasive functional brain mapping modality that combines neurophysiological data derived via electroencephalography (EEG) with magnetic resonance imaging (MRI) scans to identify brain structures and their function [15]. The procedure relies on evoked potentials (EPs) resulting from sensory stimulation.

Neurophysiological recordings, and in particular EPs, are often contaminated by noise. This may include environmental sources, like 60-Hz electrical interference, and biological sources of non-neuronal origin, like the heart activity (ECG), eye blinks, respiratory artifacts, and muscle activity. All these artifacts and the activity not contributing to a particular response result in distorted EP components, which, in turn, result in reduced source localization accuracy. To minimize the noise effects of extraneous activity, most of the published studies have used ensemble averaging to improve the signal-to-noise ratio of individual components.

This approach, however, does not provide information on the dynamics of the brain processes underlying the surface recordings. Single-trial analysis, on the other hand, can provide information on the temporal evolution of the neurophysiological processes associated with the particular EP components under investigation.

Ideally, one would like to record only the activity of the cortical generators activated by the experimental task. Recently, blind source separation procedures and, in particular, independent component analysis (ICA) has been successfully applied to EEG/EP analysis [10, 13]. These procedures are based on two main hypotheses [10], namely that the EEG data recorded at multiple scalp sensors are linear sums of temporal independent components arising from spatially fixed brain networks, and that volume conduction of electric currents from the various cortical sources does not involve significant time delays.

We have recently proposed an methodology for single-trial EP analysis [16]. The technique focuses only on a particular EP component at a time that is made visible on each single trial. Our method is based on ICA and the idea that activity resulting from an experimental stimulus is independent from neurophysiological artifacts and background brain activity [9, 10, 13]. The advantage of the method is twofold: it can extract individual components out of the entire EP waveform, and it can also provide clear estimates of these components in single trial responses. Thus, the method allows studying the dynamic evolution of the underlying cortical generators that give rise to a specific EP component.

In this paper, we tested two hypotheses: 1) improved EP estimates can provide increased source localization accuracy, and 2) the in-phase and out-of-phase partial EPs represent different processes and are generated by distinct brain structures.

II. Methods

A. Iterative ICA

Independent component analysis [3] is a method for solving the blind source separation problem [7], which tries to recover N independent source signals, $\mathbf{s} = \{s_1,\ldots,s_N\}$, from N observations, $\mathbf{x} = \{x_1,\ldots,x_N\}$, that represent linear mixtures of the independent source signals. The key assumption used to separate sources from mixtures is that the sources are statistically independent, while the mixtures are not. Mathematically, the problem is described as $\mathbf{x} = \mathbf{As}$, where $\mathbf{A}$ is an unknown mixing matrix, and the task is to recover a version, $\mathbf{u}$, of the original sources, similar to $\mathbf{s}$, by estimating a matrix, $\mathbf{W}$, which inverts the mixing process, i.e., $\mathbf{u} = \mathbf{Wx}$. The estimates $\mathbf{u}$ are called independent components (ICs). The extended infomax algorithm is currently the most efficient technique to solve this problem

and relies on information theory and a neural network approach [1, 4, 7, 8].

Our technique, termed iterative ICA (*i*ICA), is an iterative implementation of this algorithm and is applied to a set of recordings consisting of L single trials obtained from N recording channels. Before processing, all single trials are bandpass filtered between 15 and 50 Hz. The procedure consists in the following steps:

1. Compute an average EP from all single trials.
2. Compute the ICA transform of all single trials, grouped in blocks of 10.
3. Compute the absolute correlation value between the current average EP and the ICs in all blocks, within a predefined window W_r.
4. Set to zero those ICs with correlation less than a predefined threshold r_{th}.
5. Compute the inverse ICA transform of the updated ICs back to the time domain, separately in each block.
6. Shuffle the updated single trials around the entire set.
7. Repeat steps 1 to 6 until a convergence criterion is met.

The same procedure is then applied to the rest of the channels until all of them have been processed. The parameter values used in the present study were W_r = 50–250 ms poststimulus, which was consistent with the occurrence of the N100 waveform, and r_{th} = 0.15. Shuffling of the trials guarantees that each of the blocks will include different trials in the next iteration, and thus the resulting ICA system of equations will not be underdetermined.

B. Data

Data from 13 normal subjects (11 right-handed and two left-handed adults, 9 males and 4 females, ages between 23 and 42 years) were recorded with a whole-head, 256-channel, dense-array EEG (*d*EEG) scanner, using an electrode cap covering the entire head (BioSemi Active Two EEG system). The stimuli consisted of 1-kHz tones with duration of 40 msec, and 10 msec rise and fall times. Stimuli were delivered binaurally at the rate of 1.1 stimuli per second**.** The data were referenced to the linked mastoids.

C. Data Analysis

The *i*ICA method was applied to each channel separately. The processed single trials were separated into two groups: an “in-phase” one, with trials in which the N100 component had the same phase as the average response, and an “out-of-phase” one, with trials having the opposite phase [6]. Then, all trials in a particular group were averaged together to produce a partial EP. Finally, source localizations were obtained using the original unprocessed EPs, the *i*ICA-processed ensemble average EPs, and the two partial EPs. In all cases, out of the entire waveform we localized only the N100 component.

D. Source Localization

The location of the recording electrodes was digitally identified in 3D space using a Polhemus device. Equivalent current dipole (ECD) fitting of the EEG data was done in a three-sphere head model, using Curry 4.5 software. The dipole parameters were determined so that they explained the measured data optimally in the least-squares sense. The location and size of the spheres were determined individually for each subject by fitting a sphere to the measured electrode locations. For the three-shell model, the diameter of the skull, scalp, and brain was taken to be 10, 9, and 7 cm, respectively, while their conductivities were postulated to be 0.33, 0.0042 and 0.33 mho/m, respectively [2]. In all cases, we used two moving dipoles with mirror constraints to fit the N100 component, i.e., two nearly bilaterally symmetric locations in the two hemispheres [5, 10, 11, 13]. The resulting dipoles were overlaid onto each subject’s MRI.

III. RESULTS

Figure 1 shows an example of the responses obtained from a typical subject to illustrate the denoising performance of the new *i*ICA procedure. The top panel shows superimposed the original EPs obtained from all 256 channels after lowpass filtering between 0.1 and 20 Hz.

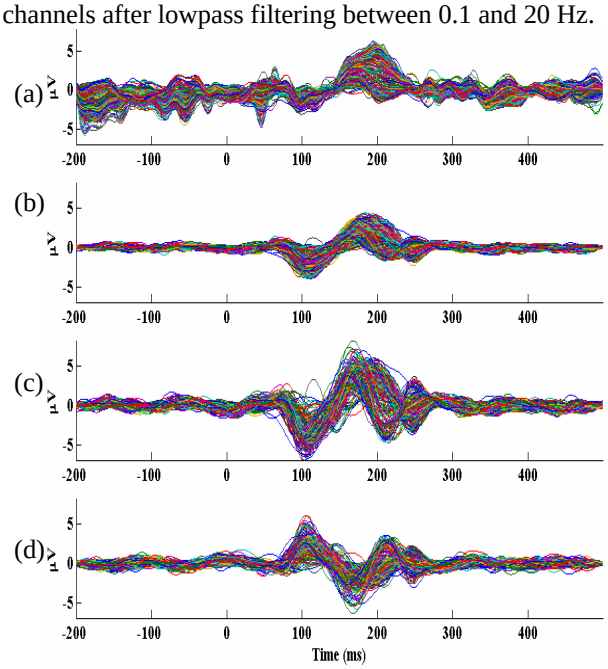

Fig. 1. Improved average EP estimates using the *i*ICA procedure. (a) Original EPs; (b) *i*ICA processed EPs, and the corresponding (c) in-phase and (d) out-of-phase partial EPs.

A clear N100 is difficult to discern in these responses due to the additional activity around this component. Figure 1 (b) shows the same responses after *i*ICA processing. In this case, the overall component morphology is improved with respect to the background activity. In particular, the N100-P200 complex is more prominent, while the surrounding activity is now drastically reduced.

Each trace in this graph resulted from averaging all *i*ICA-denoised trials corresponding to that channel, while Figure 1 (c) and (d) show the corresponding in-phase, and out-of-phase partial EPs, respectively. As it can be seen, the N100 component in these EPs is also very prominent. In addition, it has about the same amplitude, but exactly opposite phase.

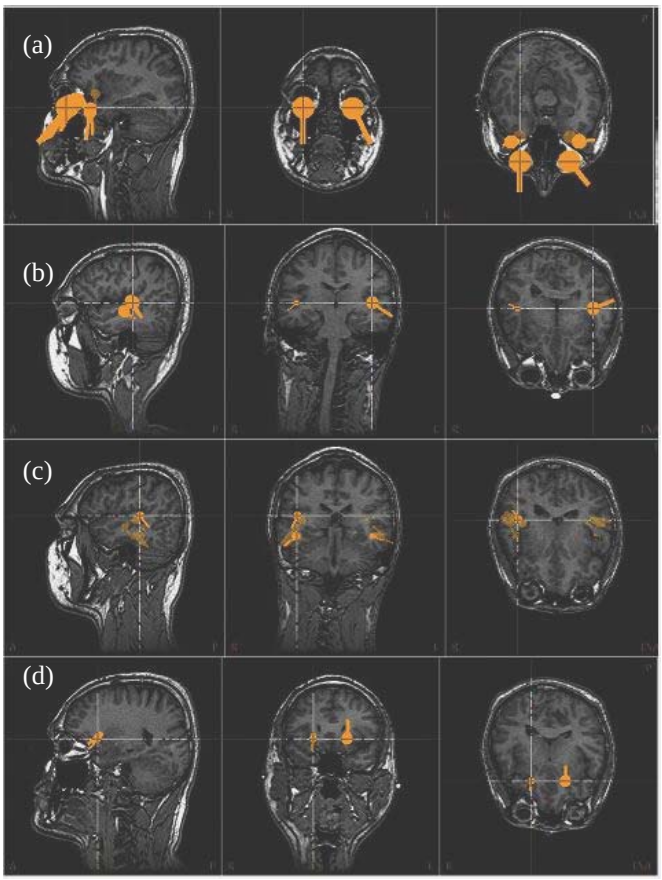

Fig. 2. Localizations obtained using the (a) original EPs, the (b) *i*ICA processed EPs, and the corresponding (c) in-phase and (d) out-of-phase partial EPs.

Figure 2 illustrates the effectiveness of the iterative ICA procedure in obtaining improved source localizations. The top panels (a) depict the source localizations obtained from the original unprocessed data when projected on sagittal, coronal, and axial sectional views. The dipolar sources indicated by yellow poles are far away from the expected actual N100 source location, which is mostly the floor of the Sylvian fissure. The sources obtained after *i*ICA processing are shown in panels (b), whereby all dipoles clearly fall on the expected areas. Multiple dipoles seem to show a successive the activation of adjacent cortical areas over time.

The dipoles depicted on panels (c) of Figure 2 are computed after fitting the N100 component using only the in-phase responses. In nine out of 13 subjects these responses provided the best localizations, especially in cases where the localizations obtained using all responses were not at the expected areas. Panels (d) of the same figure depict the sources identified after fitting the N100 component in the out-of-phase trials. The locations of these dipoles varied widely from dataset to dataset and did not follow any consistent pattern across the subjects analyzed.

IV. DISCUSSION

Results from the 13 subjects analyzed so far show that improved EPs can be obtained using the new *i*ICA procedure in terms of overall component morphology–after processing the N100 component was more prominent and better defined with respect to the background activity.

The sources of the auditory N100 component have been consistently identified in the primary auditory cortex by a variety of neuroimaging studies using evoked potentials and evoked fields [5, 11, 12, 14]. However, oftentimes extraneous activity may result in mis-localization of the sources. In our case, before processing, only four out of the 13 *d*EEG datasets could be localized correctly, whereas, after processing, in all 13 datasets the N100 sources fell clearly in the area of the primary auditory cortex, i.e., the floor of the Sylvian fissure. Further analysis showed that in most datasets the improved localizations were mostly due to the in-phase partial EPs, whereas the contribution from the out-of-phase partial EPs had an antagonistic effect. At present, the significance of this component is unknown.

In addition to accurate localizations, the iteratively processed data revealed another interesting aspect. It seemed to confirm previous evidence for a dynamic process involving successive excitation of adjacent cortical sources that are arranged along the anteroposterior axis in the auditory cortices and following the course of the supratemporal plane [14].

The above results support our hypotheses that improved response estimates result in improved source localizations, and suggest that the method can be used in clinical applications.

ACKNOWLEDGMENT

This work is supported by a training fellowship from the W.M. Keck Foundation to the Gulf Coast Consortia through the Keck Center for Computational and Structural Biology and a grant from the Texas Learning and Computation Center at the University of Houston.

REFERENCES

[1] A. Bell and T. Sejnowski, "An information-maximization approach to blind source separation and blind deconvolution," *Neural Computation*, 6:1129-59, 1995.

[2] D. Cohen, B. N. Cuffin, K. Yonokuchi, R. Maniewsk, C. Purcell, G. R. Cosgrove, I. Ives, J. G. Kennedy, and D. L. Schomer, "MEG versus EEG localization test using implanted sources in the human brain", *Annals of neurology*, 28(6): 811-817, 1990.

[3] P. Comon, "Independent component analysis—a new concept?" *Signal Proc*, 36: 287–314, 1994.

[4] M. Girolami, "An alternative perspective on adaptive independent component analysis algorithms," *Neural Computation*, 10: 2103-2114, 1998.

[5] M. Huotilainen, I. Winkler, K. Alho, C. Escera, J. Virtanen, R. J. Ilmoniemi, I.P. Jaaskelainen, E. Pekkonen, R. Naatanen, "Combined mapping of human auditory EEG and MEG responses", *Electroenceph Clin Neurophysiol*, 108(4): 370-379, 1998.

[6] D. Iyer and G. Zouridakis, "EEG and MEG phase maps using iterative independent component analysis", 22nd Annual Houston Conference on Biomedical Engineering Research, February 11-13, 2005.

[7] C. Jutten and J. Herault, "Blind separation of sources I. An adaptive algorithm based on neuromimetic architecture", *Signal Processing*, 24: 1–10, 1991.

[8] T. W. Lee, M. Girolami, T. J. Sejnowski, "Independent component analysis using an extended infomax algorithm for mixed sub-Gaussian and super-Gaussian sources". *Neural Comput.*, 11: 417-441, 1999.

[9] S. Makeig, M. Westerfield, T-P. Jung, J. Covington, J. Townsend, T. J. Sejnowski, E. Courchesne, "Independent components of the late positive response complex in a visual spatial attention task," *J Neurosc,i* 19: 2665–2680, 1999.

10] S. Makeig, M. Westerfield, T-P. Jung, S. Enghoff, J. Townsend, E. Courchesne, T. J. Sejnowski, "Dynamic brain sources of visual evoked responses", *Science*, 295: 690-694, 2002.

[11]S. Ohtomo, N. Nakasato, A. Kanno, K. Hatanaka, R. Shirane, K. Mizoi, T. Yoshimoto, "Hemispheric asymmetry of the auditory evoked N1m response in relation to the crossing point between the central sulcus and Sylvian fissure", *Electroenceph Clin Neurophysiol*., 108(3): 219-25, 1998.

[12] M. Scherg, J. Vajsar and T. W. Picton, "A source analysis of the late human auditory evoked potentials", *Journal of Cognitive Neuroscience*, 1: 336-355, 1989.

[13] R. N. Vigario, "Extraction of ocular artifacts from EEG using independent component analysis", *Electroenceph Clin Neurophysiol*, 103: 395- 404, 1997.

[14] G. Zouridakis, P. G. Simos, A. C. Papanicolaou, "Multiple bilaterally asymmetric cortical sources account for the auditory N1m component," *Brain Topogr*, 10(3): 183-189, 1998.

[15] G. Zouridakis, D. Iyer, "Functional Brain Mapping through Intracranial Source Imaging," In Biomedical Technology and Devices Handbook, J. E. Moore, Jr. and G. Zouridakis (Eds), CRC Press, 2003.

[16] G. Zouridakis, D. Iyer, "Improved Estimation of Evoked Potentials Using an Iterative Independent Component Analysis Procedure", WSEAS Transactions on Signal Processing, Robotics and Automation, 2(1): 2004